This paper is dedicated to Prof. Francesco A. Costabile on the occasion of his 70th birthday

An augmented MFS approach for brain activity reconstruction

Guido Ala[a], Gregory E. Fasshauer[b], Elisa Francomano[c], Salvatore Ganci[a], Michael J. McCourt[d]

[a]*DEIM, Università degli Studi di Palermo, Viale delle Scienze, Edificio 9, 90128 Palermo, Italy*
[b]*Department of Applied Mathematics and Statistics, Colorado School of Mines, 1500 Illinois St., Golden, CO 80401*
[c]*DIID, Università degli Studi di Palermo, Viale delle Scienze, Edificio 6, 90128 Palermo, Italy*
[d]*SigOpt, 100 Bush St., Suite 510, San Francisco, CA, 94104*

Abstract

Weak electrical currents in the brain flow as a consequence of acquisition, processing and transmission of information by neurons, giving rise to electric and magnetic fields, which can be modeled by the quasi-stationary approximation of Maxwell's equations. Electroencephalography (EEG) and magnetoencephalography (MEG) techniques allow for reconstructing the cerebral electrical currents and thus investigating the neuronal activity in the human brain in a non-invasive way. This is a typical electromagnetic inverse problem which can be addressed in two stages. In the first one a physical and geometrical representation of the head is used to find the relation between a given source model and the electromagnetic fields generated by the sources. Then the inverse problem is solved: the sources of measured electric scalar potentials or magnetic fields are estimated by using the forward solution. Thus, an accurate and efficient solution of the forward problem is an essential prerequisite for the solution of the inverse one. The authors have proposed the method of fundamental solutions (MFS) as an accurate, efficient, meshfree, boundary-type and easy-to-implement alternative to traditional mesh-based methods, such as the boundary element method and the finite element method, for computing the solution of the M/EEG forward problem. In this paper, further investigations about the accuracy of the MFS approximation are reported. In particular, the open question of how to efficiently design a good solution basis is approached with an algorithm inspired by the Leave-One-Out Cross Validation (LOOCV) strategy. Numerical results are presented with the aim of validating the augmented MFS with the state-of-the-art BEM approach. Promising results have been obtained.

Keywords: Method of Fundamental Solutions, Boundary value problems, M/EEG, LOOCV algorithm

Email addresses: `guido.ala@unipa.it` (Guido Ala[a]), `fasshauer@mines.edu` (Gregory E. Fasshauer[b]), `elisa.francomano@unipa.it` (Elisa Francomano[c]), `salvatore.ganci@unipa.it` (Salvatore Ganci[a]), `mccourt@sigopt.com` (Michael J. McCourt[d])

1. Introduction

Nowadays, several different technologies are available for human brain imaging. Anatomy of the brain can be investigated by computed tomography (CT) [24] and magnetic resonance imaging (MRI) [9], which provide high resolution images. However, other imaging techniques are required to obtain information on the brain activity.

This task can be performed with high spatial accuracy, in the order of a few millimeters, by means of nuclear imaging methods, such as positron emission tomography (PET) [31], the single photon emission computed tomography (SPECT) [25], and the functional magnetic resonance imaging (fMRI) [7], which are related to changes of blood flow or oxygen transportation in the brain. The temporal resolution of PET and SPECT is in the order of seconds. fMRI data might be acquired with a resolution of 100 ms, but properties of the blood flow practically limit the temporal resolution to 1 s.

A better temporal resolution can be obtained by using electromagnetic imaging techniques. In fact, acquisition, processing and transmission of information by neurons generate weak electrical currents flowing in the human brain: electroencephalography (EEG) and magnetoencephalography (MEG) can be used to obtain a better temporal resolution, in the order of 1 ms, with typical spatial resolutions in the order of 1 cm. In addition, the electromagnetic techniques are non-invasive, whereas, in nuclear imaging techniques, severe limitations are imposed by the maximum radiation dose that is admissible in order to safeguard the patient.

Electric potential and magnetic field distributions can be measured by means of an array of electrodes on the scalp, for EEG, or superconducting quantum interference devices (SQUID), for MEG, located near the head. EEG can detect activity both in the *sulci* and at the top of the cortical *gyri*, whereas MEG is most sensitive to activity originating in sulci and provides a better spatial resolution [20]. An inverse problem must be solved to estimate the neuronal activity sources corresponding to a set of measured data (electric potential or magnetic fields).

The solution of this inverse problem requires an accurate forward solver. Such a numerical tool computes the scalp potential and/or magnetic fields generated by a set of current sources representing the neural activity, given knowledge of both the physical properties of the biological tissues and the geometry of the head [19]. The efficient solution of the M/EEG forward problem is investigated in this paper.

So far, the M/EEG forward problem has been addressed by traditional mesh-based numerical methods [19]. Among these methods, the Boundary Element Method (BEM) [21, 45, 26] is the common choice because of its efficiency with respect to the Finite Elements Method (FEM) [44, 8, 43]. In particular, the symmetric Galerkin BEM is currently implemented in widely used software packages for M/EEG source analysis [32, 39]. However, the BEM involves costly numerical integration, requires an often nontrivial meshing of the domain boundaries at high quality and could potentially introduce mesh-related artifacts in the reconstructed neural activation pattern. The forward solver needs to be accurate and fast in order to act as an efficient component within an inverse solver.

To this aim, the meshless Method of Fundamental Solutions (MFS) [13] has been proposed by the authors [3, 4] for solving the boundary value problem (BVP) which arises in the M/EEG context. The MFS approximates the solution of the given BVP by a linear combination of fundamental solutions of the governing PDE. Each of these basis functions which serve as a component of the linear combination is defined by a *kernel center* located on a fictitious boundary outside the physical domain. The coefficients of the linear combination are determined by enforcing the boundary conditions at a set of *collocation points* on the true physical boundary.

Unlike many other numerical methods, normals to interfaces and pairwise distances between points are the only geometric quantities that are needed, so the MFS is meshfree and, in terms of computational time, benefits from the elimination of the meshing task in the pre-processing stage. A reduction of CPU time can also be obtained, with respect to the state-of-the-art Galerkin BEM, in the process of assembling the system matrix. This advantage plays an important role when applying the forward solver within the iterative solution of the inverse problem. Further benefits come from the ease of implementation, which makes computer codes very flexible in contrast to mesh-based solvers.

This paper investigates strategies to improve the accuracy of the MFS approximation without a decrease in efficiency. It has already been established that the accuracy of the MFS approximation does depend on the location of the centers [11]: indeed, finding a practical and efficient way of answering the question of how to pick the centers remains an open problem in the MFS context. In this paper, we approach the determination of center locations by using a strategy inspired by the leave-one-out cross validation (LOOCV) algorithm, which originates in the statistics literature [35] and which has been successfully applied also in the MFS context [10].

The paper is organized as follows. In Section 2 the state of the art of the M/EEG forward solution is summarized. In Section 3 the MFS solver for the M/EEG context is discussed. The LOOCV-like approach is presented in Section 4. In Section 5, numerical results are analyzed for a realistic single-shell head geometry, by addressing numerical accuracy, convergence and computational load comparing them with a state-of-the-art Galerkin BEM solver. A brief conclusion completes the paper.

2. State of the art of the M/EEG forward solution

Grid based numerical methods (FEM, BEM) are usually adopted in solving PDEs that model problems in engineering and science. These methods are often based on the discretization of the whole problem domain (FEM), using a mesh to support the local approximation. For problems in complicated geometries, the mesh generation is a time-consuming and costly process, even when automatic algorithms are used.

Wherever possible, boundary-type methods which require only a boundary discretization, may be preferred. Hence, BEM has been widely used, even if it may introduce drawbacks in the mathematical formulation of the problem and in the numerical integration of singular functions. Even without the need to discretize a 3D volume, the meshing of 3D surfaces is still a non-trivial task.

In the last decades, meshfree methods have been proposed and applied in many fields [14]. Meshfree methods allow for the numerical solution of PDEs without a predefined problem domain mesh: the approximation is performed only by nodes that are distributed in the problem domain, without any underlying connection between them. Among these methods, kernel-based collocation methods [15] have recently received great attention.

The main idea of kernel-based approximation methods is to estimate the solution of the given BVP by means of a linear combination of so-called *kernel* functions, which are defined using a set of points named *centers*. The differential equation and the boundary conditions are enforced at a discrete set of points named *collocation points*.

So far, traditional mesh-based methods, such as FEM [44, 8, 43, 40, 42] and BEM [22, 21, 45, 26], have been implemented to address the EEG forward problem in domains generated by realistic head models [19]. Even though FEM can handle the most realistic head models, the BEM has become the method of choice for many practical applications.

The success of the BEM in M/EEG forward solving is mainly due to its nature as a boundary-type method: not only does it avoid cumbersome and computationally expensive pre-processing 3D mesh generation, but it also has low computational cost when compared to the FEM for a given head model and desired numerical accuracy [1], since it requires computation only on the boundaries. Currently, the symmetric Galerkin BEM proposed in [26] can be considered the state-of-the-art method for solving the M/EEG forward problem. This method is implemented in the OpenMEEG library, which has been adopted by various widely used software packages [32, 39]. In the symmetric Galerkin BEM approach, both the electric scalar potential and its normal derivative on the interfaces are unknown. Linear and constant functions are used to approximate the potential and its normal derivative on the interfaces, respectively, and the residual minimization is carried out by a mixed integral approach, i.e., by using constant weights for the potential and linear weights for its normal derivative.

The difficulties in handling the geometric complexity of biological structures motivated the recent incorporation of meshfree methods in M/EEG research. In [41], the finite points mixed method (FPMM) is proposed as a meshfree method for solving the EEG forward problem. In [2, 5], the smoothed particle hydrodynamics (SPH) method is reformulated to be applied to the MEG forward problem. However, these methods require computational nodes distributed in the entire domain; therefore, though they avoid both the mesh generation step in pre-processing and costly numerical integration in assembling the system matrix, BEM solvers may outperform them in a computational cost per accuracy comparison [41].

3. MFS modeling of brain activity

In order to solve the MEG problem, posed as a set of coupled BVPs for the 3D Laplace operator, a head model consisting of nested regions with piecewise-constant conductivity is formulated. Let L be the number of nested regions in the domain Ω that represents the head, Ω_ℓ be the generic region with outer (toward the air outside the body) boundary $\partial\Omega_\ell$ and conductivity σ_ℓ, and let $I_{\ell,\ell+1} = \partial\Omega_\ell \cap \partial\Omega_{\ell+1}$ be the interface between the region ℓ and the region $\ell + 1$. The region Ω_{L+1} surrounding the head corresponds to the ambient air which is unbounded and has negligible conductivity.

The problem can be formulated as the following set of BVPs coupled by interface conditions:

$$\begin{cases} \sigma_\ell \nabla^2 \phi_\ell(\mathbf{p}) = S_\ell(\mathbf{p}) & \mathbf{p} \in \Omega_\ell \\ \phi_\ell(\mathbf{p}) = \phi_{\ell+1}(\mathbf{p}) & \mathbf{p} \in I_{\ell,\ell+1}|_{\ell \neq L} \quad \ell = 1, \dots, L \\ \sigma_\ell \mathbf{n}(\mathbf{p}) \cdot \nabla\phi_\ell(\mathbf{p}) = \sigma_{\ell+1}\mathbf{n}(\mathbf{p}) \cdot \nabla\phi_{\ell+1}(\mathbf{p}) & \mathbf{p} \in I_{\ell,\ell+1} \end{cases} \quad (1)$$

where ϕ_ℓ is the electric scalar potential in the ℓ-th region, $\mathbf{n}(\mathbf{p})$ denotes the outward unit normal vector to the interface $I_{\ell,\ell+1}$ at $\mathbf{p}$ and the source term $S_\ell(\mathbf{p})$ can be expressed as follows:

$$S_\ell(\mathbf{p}) = \begin{cases} \nabla \cdot (\mathbf{Q}\delta(\mathbf{p} - \mathbf{p}')) & \text{source at } \mathbf{p}' \in \Omega_\ell \\ 0 & \text{otherwise.} \end{cases} \quad (2)$$

The quantity $\mathbf{Q}\delta(\mathbf{p} - \mathbf{p}')$ is the source current density modeling a single neural source, for the sake of simplicity. It can be viewed as a current dipole of moment $\mathbf{Q}$ located at $\mathbf{p}' \in \Omega$. By applying the superposition principle, the general case of many dipoles can be straightforwardly addressed.
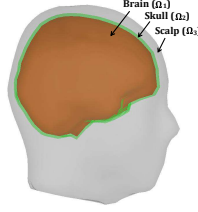
Figure 1. Three regions (brain, skull and scalp) head model.

In considering a certain region independently, it is clear that the governing PDE is a Poisson equation if a neural source is located in that region or a Laplace equation otherwise. A model with three nested regions (brain, skull and scalp) is common for the EEG problem (Figure 1). However, other regions could be added to improve the model of the head, e.g., cerebrospinal fluid and/or distinct regions for gray and white matter. Anyway, a homogeneous model of the high-conductivity brain compartment is sufficient to solve the MEG forward problem [21, 38]. The authors have proposed the Method of Fundamental Solutions (MFS) [3, 4] for solving the M/EEG forward problem. The MFS has been applied to various physical problems and its simplicity and ease of implementation make the method itself quite popular.

The MFS is a kernel-based boundary-type method which can be applied when a fundamental solution of the PDE is known. The MFS method gives the solution u of the given homogeneous BVP by a linear combination of *fundamental solutions* K of the governing homogeneous PDE, i.e.,

$$u(\mathbf{p}) = \sum_{\xi_j \in \Xi} c_j K(\mathbf{p}, \xi_j), \quad \mathbf{p} \in \Omega, \tag{3}$$

where:

$$K(\mathbf{p}, \xi_j) = \frac{1}{4\pi \|\mathbf{p} - \xi_j\|} \tag{4}$$

is the fundamental solution of the Laplace operator and $\Xi = (\xi_j)_{j=1}^{N}$ is a set of *centers* located on a *fictitious boundary* outside the physical domain Ω in order to avoid the singularities of K in the representation of the solution. The coefficients of the combination are determined by enforcing it to satisfy the boundary conditions [3, 4] by means of a collocation procedure at a set P of *collocation points*.

In applying the MFS, a fictitious boundary location strategy has to be considered. A natural choice is to conveniently inflate/deflate the physical boundary with respect to its centroid [3, 4]. The standard MFS formulation coupled with this simple heuristic method for the placement of the fictitious boundaries provides an acceptable accuracy while maintaining a low computational cost. This is a relevant task in integrating the forward solver into the inverse problem context to determine the dipole sources location.

The governing PDE of the M/EEG forward problem in the region ℓ may be homogeneous or inhomogeneous depending on the absence or the presence of a neural source in the region. While MFS can be applied directly in the former case, in the latter case an inhomogeneous problem can be reduced to a homogeneous one by the method of particular solution (MPS), i.e., by considering the solution u as the sum of a particular solution u_p and its associated homogeneous solution u_h, i.e.,

$$u = u_h + u_p. \tag{5}$$

Then one gets the following homogeneous BVP for u_h:

$$\begin{cases} Lu_h(\mathbf{p}) = f^\Omega(\mathbf{p}) - Lu_p(\mathbf{p}) = 0, & \mathbf{p} \in \Omega, \\ Tu_h(\mathbf{p}) = f^{\partial\Omega}(\mathbf{p}) - Tu_p(\mathbf{p}), & \mathbf{p} \in \partial\Omega, \end{cases} \tag{6}$$

where L is an elliptic differential operator, $\partial\Omega$ is the boundary of the domain Ω, and T and $f^{\partial\Omega}$ are the operator and the function that define the boundary conditions, respectively. Therefore, if u_p is known, u can be estimated by approximating the term u_h via the MFS by using M collocation points and N centers, with $M > N$ [3] ; the case $M = N$ is also standard for MFS methods [13], but we restrict to the $M > N$ case here to build on the format set forth in [4] and help ensure greater stability [37].

The collocation, enforced on each interface, generates an overdetermined linear system $A\mathbf{c} = \mathbf{b}$ which is solved in the least squares sense. To this aim, a set $P_{\ell,\ell+1}$ of collocation points on the interface $I_{\ell,\ell+1}$ and a set of centers Ξ_ℓ are considered. In particular, for a head model with three nested compartments ($L = 3$), we get

$$A = \begin{pmatrix} A_{1,2}^{(1)} & A_{1,2}^{(2)} & \\ & A_{2,3}^{(2)} & A_{2,3}^{(3)} \\ & & \hat{A}_{3,4}^{(3)} \end{pmatrix}, \qquad \mathbf{c} = \begin{pmatrix} \mathbf{c}^{(1)} \\ \mathbf{c}^{(2)} \\ \mathbf{c}^{(3)} \end{pmatrix}, \qquad \mathbf{b} = \begin{pmatrix} \mathbf{b}_{1,2} \\ \mathbf{b}_{2,3} \\ \hat{\mathbf{b}}_{3,4} \end{pmatrix}, \tag{7}$$

where the superscripts are directly related to the interfaces (eq. 1). In (7), the blocks of the matrix A collect the continuity of the electric scalar potential and the normal component of the current density imposed at the collocation points which we refer to as $\mathbf{p}_i \in P_{\ell,\ell+1}^D$ and $\mathbf{p}_i \in P_{\ell,\ell+1}^N$ respectively,

$$A_{\ell,\ell+1}^{(s)} = \begin{pmatrix} D_{\ell,\ell+1}^{(s)} \\ N_{\ell,\ell+1}^{(s)} \end{pmatrix} \qquad \ell = 1, 2; s = \ell, \ell + 1, \tag{8}$$

with

$$\begin{aligned} (D_{\ell,\ell+1}^{(s)})_{i,j} &= (-1)^{s+1} K(\mathbf{p}_i, \boldsymbol{\xi}_j) & \mathbf{p}_i \in P_{\ell,\ell+1}^D, \ \boldsymbol{\xi}_j \in \Xi_\ell, \\ (N_{\ell,\ell+1}^{(s)})_{i,j} &= (-1)^{s+1} \sigma_\ell \mathbf{n}(\mathbf{p}_i) \cdot \nabla K(\mathbf{p}_i, \boldsymbol{\xi}_j) & \mathbf{p}_i \in P_{\ell,\ell+1}^N, \ \boldsymbol{\xi}_j \in \Xi_\ell, \end{aligned}$$

and the last block comprised of only the values

$$(\hat{A}_{3,4}^{(3)})_{i,j} = \sigma_3 \mathbf{n}(\mathbf{p}_i) \cdot \nabla K(\mathbf{p}_i, \boldsymbol{\xi}_j) \qquad \mathbf{p}_i \in P_{3,4}^N, \ \boldsymbol{\xi}_j \in \Xi_3.$$

The blocks of the known vector are

$$\mathbf{b}_{\ell,\ell+1} = \begin{pmatrix} \mathbf{b}_{\ell,\ell+1}^D \\ \mathbf{b}_{\ell,\ell+1}^N \end{pmatrix} \qquad \ell = 1, 2, \tag{9}$$

with

$$\begin{aligned} (\mathbf{b}_{\ell,\ell+1}^D)_i &= \alpha_{\ell+1} \phi_{p,\ell+1}(\mathbf{p}_i) - \alpha_\ell \phi_{p,\ell}(\mathbf{p}_i) & \mathbf{p}_i \in P_{\ell,\ell+1}^D, \\ (\mathbf{b}_{\ell,\ell+1}^N)_i &= \alpha_{\ell+1} \sigma_{\ell+1} \mathbf{n}(\mathbf{p}_i) \cdot \nabla \phi_{p,\ell+1}(\mathbf{p}_i) - \alpha_\ell \sigma_\ell \mathbf{n}(\mathbf{p}_i) \cdot \nabla \phi_{p,\ell}(\mathbf{p}_i) & \mathbf{p}_i \in P_{\ell,\ell+1}^N, \end{aligned}$$

and, on the external interface,

$$(\hat{\mathbf{b}}_{3,4}^N)_i = -\alpha_3 \sigma_3 \mathbf{n}(\mathbf{p}_i) \cdot \nabla \phi_{p,3}(\mathbf{p}_i), \qquad \mathbf{p}_i \in P_{3,4}^N.$$

In the previous formulas the subscript p of the electric scalar potential refers to the particular solution (eq. 5), and the following position holds (Figure 1):

$$\alpha_\ell = \begin{cases} 1, & \text{neural source in } \Omega_\ell, \\ 0, & \text{otherwise.} \end{cases} \tag{10}$$

An analogous procedure has been proposed for solving the EEG forward problem both in the FEM [8, 42] and in some meshfree context [41, 2].

Once the scalar electric potential distribution is obtained, the forward problem for the magnetic flux density can be evaluated. In fact, the magnetic flux density $\mathbf{B}$ at a point $\mathbf{p}$ outside Ω can be determined by means of the Ampère-Laplace-Biot-Savart law and a corollary of the Divergence Theorem [36, 20]:

$$\mathbf{B}(\mathbf{p}) = \mathbf{B}_s(\mathbf{p}) + \frac{\mu}{4\pi} \sum_{\ell=1}^{L} (\sigma_{\ell+1} - \sigma_\ell) \int_{I_{\ell,\ell+1}} \phi(\mathbf{p}^*)\, \mathbf{n}(\mathbf{p}^*) \times \frac{\mathbf{p} - \mathbf{p}^*}{\|\mathbf{p} - \mathbf{p}^*\|^3}\, \mathrm{d}s, \tag{11}$$

where $\mathbf{B}_s(\mathbf{p})$ is an analytical term:

$$\mathbf{B}_s(\mathbf{p}) = \frac{\mu}{4\pi} \mathbf{Q} \times \frac{\mathbf{p} - \mathbf{p}'}{\|\mathbf{p} - \mathbf{p}'\|^3}. \tag{12}$$

So the crucial point is to efficiently evaluate the scalar electric potential distribution.

4. Augmented MFS approach

Despite the simplicity and easy implementation of the MFS, there are some important issues of the method which have not yet been satisfactorily addressed. In particular, as already pointed out, the accuracy of the MFS approximation depends on the location of the centers, and picking the centers in a *practical* and *efficient* way is still an open problem. For example, in the scientific literature [10] it has been emphasized that the stability of the MFS in an analytic domain is controlled by the singularities in the analytic continuation of the solution. However, for non-analytic boundary or data, and in coupled settings (e.g. M/EEG problems), there is still no way to determine the location of the singularities in the analytic continuation of the solution. In this paper we address this issue, namely how to choose the location of the sources in a satisfactory way, though perhaps not an optimal one, in order to obtain augmented results when the MFS is applied to M/EEG problems.

In the scientific literature two approaches are proposed. The first one is a dynamic one: the center coordinates are determined along with the coefficients of the MFS expansion by costly nonlinear least-squares solvers [28, 23]. Alternatively, in the static approach, the centers are pre-assigned by, e.g., inflating/deflating the physical interfaces/boundaries or projecting the collocation points along the surface normals. These normals must be approximated, which we did using the raw mesh; this could be improved using a higher quality approximation to the surface from the point cloud data [34]. In a two-dimensional domain, uniform distribution of the collocation points around the boundary and the placement of the kernel centers on a pseudo-boundary congruent to the physical boundary produces the most accurate and stable results. In a three-dimensional domain, the uniform distribution of the collocation points on the surface of an irregular region is not a trivial task; three-dimensional applications often produce collocation points by scanning the surface of the object [27].

Static strategies are computationally advantageous, but the location of the centers is controlled by one or more parameters, such as an inflation/deflation coefficient or a distance from the physical interface, which must be determined. In this problem we consider a single inflation/deflation coefficient η as a free parameter which defines the degree to which the actual surface is deformed into the fictitious boundary on which the kernel centers (also called the source points in MFS literature) lie. If $\mathbf{p}_i$ is a generic collocation point on the physical surface, the corresponding center $\boldsymbol{\xi}_i$ on the fictitious surface is given by:

$$\boldsymbol{\xi}_i = \mathbf{p}_i + \eta\mathbf{n}(\mathbf{p}_i). \tag{13}$$

Figure 2 provides some insight regarding the role the parameter η has in defining the collocation point and kernel center distribution.
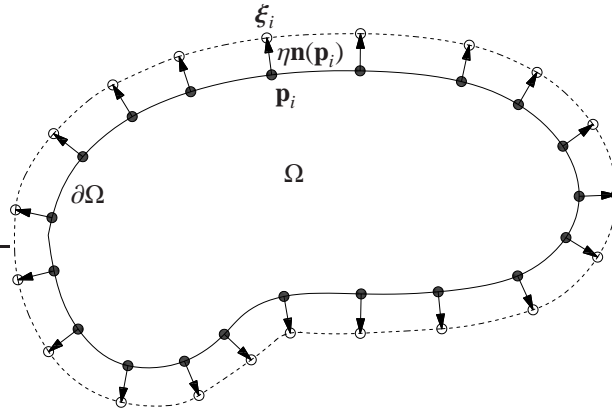
Figure 2. This computational setting involves M collocation points (●), at which the PDE is enforced, located on the brain surface. N source points (the MFS kernel centers, ○) are placed on a fictitious boundary (dashed line) outside of the domain Ω. The fictitious boundary is defined by a parameter η: larger values of η yield a greater "inflation" of the brain surface, whereas smaller values of η place the kernel center $\boldsymbol{\xi}_i$ closer to the surface (and, thus, potentially closer to the collocation point $\mathbf{p}_i$).

The following sections define two possible metrics, C_{LOO} and C_{GCV}, which measure, in some way, the quality of the solution for a given η parameter. Prior to conducting the MFS solve to determine the numerical solution to (1), the η which minimizes one of these quantities should be found (through a standard numerical optimization method such as BFGS [30]) and used to generate the solution basis for the MFS approximation to the electric scalar potential.

4.1. Leave one out cross validation

A strategy for finding a "satisfactory" parameter η is to use a *cross validation approach* which originated in the statistics literature. In particular, the leave one out cross validation (LOOCV) algorithm was proposed in [35] for optimizing the shape parameter of radial basis function (RBF) interpolation systems; later, it was used as an inspiration in [16] for solving elliptic BVPs by RBF methods. In [10] the same LOOCV-like algorithm is used in choosing the location of the sources (i.e., the centers) in the MFS context.

We modify this idea here to select the parameter η by minimizing the (least squares) error for a fit to the (boundary) data based on an MFS expansion for which one of the centers was "left out". To judge the quality of the solution as a contribution of that source center, we will

also "leave out" the corresponding collocation point from which that center was inflated/deflated. In reality, any choice of omitted collocation points is viable (including omitting more than one collocation point per term, or potentially no collocation points), but this strategy, of omitting a center and matching collocation point, is chosen to parallel the standard LOOCV strategy where those points actually coincide.

In contrast to the standard setting detailed in [10], however, our collocation matrix is no longer square, and thus has no inverse. Here we will work through the comparable derivation and identify the new aspects of this situation.

Suppose that we have the full MFS solution,

$$u(\mathbf{p}) = \sum_{j=1}^{N} c_j K(\mathbf{p}, \boldsymbol{\xi}_j), \qquad \mathbf{p} \in \Omega, \qquad \boldsymbol{\xi}_j \in \Xi, \tag{14}$$

in the region for which we have boundary data and want to determine an appropriate η inflation parameter with which to define the $\boldsymbol{\xi}_j$ locations. There are N centers $\boldsymbol{\xi}_j$ and M collocation locations $\mathbf{p}_i$, but because every point on the fictitious boundary is inflated/deflated from a point on the true boundary, we can suitably order the points so that

$$\boldsymbol{\xi}_i \text{ is the inflated point associated with } \mathbf{p}_i, \qquad 1 \le i \le N.$$

This defines a relationship between all of the kernel centers and a subset of the collocation points. The order of the remaining collocation points $\boldsymbol{p}_{N+1}, \dots, \boldsymbol{p}_M$ is immaterial.

The strategy behind LOOCV is that a collocation point for which we have boundary data is intentionally omitted from the solution (14), and the error of the resulting solution, as computed without that data, at that collocation point is a measurement of how wrong the choice of η is for that point. Accumulating these residuals at all collocation points $\mathbf{p}_i$ with corresponding centers $\boldsymbol{\xi}_i$ (each approximation omits both $\boldsymbol{\xi}_i$ and $\mathbf{p}_i$), gives a metric which judges the inappropriateness of a given choice of η. Minimizing this metric gives, in a sense, the optimal choice of η.

For each collocation point which is "left out", we have an associated permutation of the full least squares system,

$$\mathsf{K} = \begin{pmatrix} K(\mathbf{p}_1, \boldsymbol{\xi}_1) & \cdots & K(\mathbf{p}_1, \boldsymbol{\xi}_N) \\ & \vdots & \\ K(\mathbf{p}_M, \boldsymbol{\xi}_1) & \cdots & K(\mathbf{p}_M, \boldsymbol{\xi}_N) \end{pmatrix}, \tag{15}$$

isolating the points that will be used to create the approximation (called the training set) and the point at which the residual will be computed (called the validation set). This partitions K into blocks,

$$\mathsf{K} = \begin{pmatrix} \mathsf{K}_{tt} & \mathsf{K}_{tv} \\ \mathsf{K}_{vt} & \mathsf{K}_{vv} \end{pmatrix}, \tag{16}$$

where $\mathsf{K}_{tt} \in \mathbb{R}^{M-1 \times N-1}$, $\mathsf{K}_{tv} \in \mathbb{R}^{M-1 \times 1}$, $\mathsf{K}_{vt} \in \mathbb{R}^{1 \times N-1}$ and $\mathsf{K}_{vv} \in \mathbb{R}$.

In practical terms, K_{tt} represents the collocation matrix for fitting only the training set and K_{vt} represents the solution basis for evaluation at the validation points—the notation K_{vt} is meant to bolster this intuition of basis function for evaluation on the <u>v</u>alidation set and centered on the <u>t</u>raining set. This follows the same notation as appeared in [15], but here the matrix is rectangular, which poses new difficulties. If we similarly partition our least square system coefficient $\boldsymbol{c}$ and boundary data $\boldsymbol{b}$ as

$$\boldsymbol{c} = \begin{pmatrix} \boldsymbol{c}_t \\ \boldsymbol{c}_v \end{pmatrix}, \quad \boldsymbol{c} \in \mathbb{R}^N, \qquad \boldsymbol{b} = \begin{pmatrix} \boldsymbol{b}_t \\ \boldsymbol{b}_v \end{pmatrix}, \quad \boldsymbol{b} \in \mathbb{R}^M, \tag{17}$$

the full approximation problem (leaving nothing out) is

$$\mathsf{K}\boldsymbol{c} = \boldsymbol{b} \quad \Rightarrow \quad \begin{pmatrix} \mathsf{K}_{tt} & \mathsf{K}_{tv} \\ \mathsf{K}_{vt} & \mathsf{K}_{vv} \end{pmatrix} \begin{pmatrix} \boldsymbol{c}_t \\ \boldsymbol{c}_v \end{pmatrix} = \begin{pmatrix} \boldsymbol{b}_t \\ \boldsymbol{b}_v \end{pmatrix}. \tag{18}$$

Because the goal of leave one out cross validation is to determine the effectiveness of solution parameters (such as the fictitious boundary parameter η), we use the predictions on the validation set generated by solving the problem on the training set to define a residual denoted e_{vt}. If only the training set is considered, the overdetermined linear system $\mathsf{K}_{tt}\hat{\boldsymbol{c}} = \boldsymbol{b}_t$ defines the coefficients $\hat{\boldsymbol{c}}$ for prediction on the validation set; those predictions take the form $\mathsf{K}_{vt}\hat{\boldsymbol{c}}$. We can therefore define the residual at the validation point as

$$e_{vt} = \boldsymbol{b}_v - \mathsf{K}_{vt}\mathsf{K}_{tt}^+\boldsymbol{b}_t, \tag{19}$$

where K_{tt}^+ represents the pseudoinverse [18] of K_{tt}. This residual represents the accuracy for a single validation pair $\mathbf{p}_i, \boldsymbol{\xi}_i$; it is then necessary to cycle through and give all points $\boldsymbol{\xi}_i \in \Xi$ an opportunity to contribute as a validation point, so multiple such residuals are combined as

$$C_{\text{LOO}} = \sum_{\text{each validation point}} e_{vt}^2 \tag{20}$$

to form the metric C_{LOO} we hope to minimize.

Simple though that may be to state, the cost of using (19) for each point left out becomes prohibitive, since each point should, in theory, require solving a least squares problem involving an $M - 1 \times N - 1$ sized K_{tt}. For a square system, [35] demonstrated that terms appearing in K^{-1} can be reused to compute each LOOCV component residual at (nearly) no additional cost. In our current rectangular setting, we instead have the pseudoinverse $\mathsf{G} \equiv \mathsf{K}^+$, which must satisfy

$$\begin{pmatrix} \mathsf{G}_{tt} & \mathsf{G}_{vt} \\ \mathsf{G}_{tv} & \mathsf{G}_{vv} \end{pmatrix} \begin{pmatrix} \mathsf{K}_{tt} & \mathsf{K}_{tv} \\ \mathsf{K}_{vt} & \mathsf{K}_{vv} \end{pmatrix} = \begin{pmatrix} \mathsf{I}_{N-1} & \\ & 1 \end{pmatrix} \tag{21}$$

so long as K has full column rank (a prerequisite for a given η to be suitable). This identity provides

$$\mathsf{G}_{tv}\mathsf{K}_{tt} + \mathsf{G}_{vv}\mathsf{K}_{vt} = 0 \qquad \implies \qquad \mathsf{K}_{vt}\mathsf{K}_{tt}^+ = -\mathsf{G}_{vv}^{-1}\mathsf{G}_{tv}\mathsf{K}_{tt}\mathsf{K}_{tt}^+. \tag{22}$$

which can be substituted back into (19) to give a slightly different form of the residual,

$$e_{vt} = \boldsymbol{b}_v + \mathsf{G}_{vv}^{-1}\mathsf{G}_{tv}\mathsf{K}_{tt}\mathsf{K}_{tt}^+\boldsymbol{b}_t. \tag{23}$$

At this point, the distinction from the standard square K case is most obvious: in that setting, $\mathsf{K}^+ = \mathsf{K}^{-1}$ leaving $\mathsf{K}_{tt}\mathsf{K}_{tt}^+ = \mathsf{I}_{N-1}$. In the standard leave one out cross validation setting described in, e.g., [35], it is possible to reduce the cost of computing (23) by manipulating

$$\begin{pmatrix} \boldsymbol{c}_t \\ \boldsymbol{c}_v \end{pmatrix} = \mathsf{K}^+\boldsymbol{b} = \begin{pmatrix} \mathsf{G}_{tt} & \mathsf{G}_{vt} \\ \mathsf{G}_{tv} & \mathsf{G}_{vv} \end{pmatrix} \begin{pmatrix} \boldsymbol{b}_t \\ \boldsymbol{b}_v \end{pmatrix} \quad \Rightarrow \quad \boldsymbol{c}_v = \mathsf{G}_{tv}\boldsymbol{b}_t + \mathsf{G}_{vv}\boldsymbol{b}_v$$

to produce the identity

$$\mathsf{G}_{vv}^{-1}\boldsymbol{c}_v = \boldsymbol{b}_v + \mathsf{G}_{vv}^{-1}\mathsf{G}_{tv}\boldsymbol{b}_t. \tag{24}$$

These manipulations, applied to the true inverse instead of the pseudoinverse, is what allows LOOCV to maintain a reasonable cost in the square setting.

We argue that the same computation can be used in this least squares setting under reasonable conditions. In particular, we note that $\mathsf{K}_{tt}\mathsf{K}_{tt}^{+}\boldsymbol{b}_t$ is a projection of $\boldsymbol{b}_t$ into range(K_{tt}). Thus, we can write $(\mathsf{I}_{N-1}-\mathsf{K}_{tt}\mathsf{K}_{tt}^{+})\boldsymbol{b}_t = \boldsymbol{\delta}$, that is, $\boldsymbol{\delta}$ is the projection of $\boldsymbol{b}_t$ into range(K_{tt})$^{\perp}$. If we think about these components in terms of the approximation problem we are trying to solve, $\mathsf{K}_{tt}\mathsf{K}_{tt}^{+}\boldsymbol{b}_t$ represents the component of $\boldsymbol{b}_t$ which is well represented by the Green's kernel basis and $\boldsymbol{\delta}$ represents the component which cannot be effectively approximated. From this standpoint,

$$\mathsf{K}_{tt}\mathsf{K}_{tt}^{+}\boldsymbol{b}_t = \boldsymbol{b}_t - \boldsymbol{\delta}, \tag{25}$$

and therefore

$$\begin{aligned}
e_{vt} &= \boldsymbol{b}_v + \mathsf{G}_{vv}^{-1}\mathsf{G}_{tv}\boldsymbol{b}_t - \mathsf{G}_{vv}^{-1}\mathsf{G}_{tv}\boldsymbol{\delta} \\
&= \mathsf{G}_{vv}^{-1}\boldsymbol{c}_v - \mathsf{G}_{vv}^{-1}\mathsf{G}_{tv}\boldsymbol{\delta}.
\end{aligned} \tag{26}$$

If we believe that our MFS method is effectively approximating the boundary data, then the $\boldsymbol{\delta}$ term should be small (since there should be very little about the data which is left unaccounted) and could be discarded during the computation. The judgment about how small is appropriate would have to be determined by the practitioner, but a good surrogate for the magnitude of each of these LOOCV $\boldsymbol{\delta}$ terms is the residual of the full $\mathsf{K}\boldsymbol{c} = \boldsymbol{b}$ least squares problem, since the difference between the two is only a single point.

4.2. Generalized cross validation

In case the LOOCV-like formula (26) discussed above proves infeasible because the $\boldsymbol{\delta}$ term was unacceptably large to approximate as 0, it is possible to employ a *generalized cross validation* (GCV) criterion [12, 17]. The GCV criterion uses the projection matrix

$$\mathsf{P} = \mathsf{I}_M - \mathsf{K}(\mathsf{K}^T\mathsf{K})^{-1}\mathsf{K}^T \tag{27}$$

which, after some manipulations, can be expressed in terms of the pseudoinverse as

$$\mathsf{P} = \mathsf{I}_M - \mathsf{K}\mathsf{K}^{+}. \tag{28}$$

Note the similarity to the projection matrix that appeared in the LOOCV setting when attempting to approximate each LOOCV residual. For the generalized cross validation, no data is left out and the projection matrix is used to invoke the full residual by noting that $\mathsf{P}\boldsymbol{b} = \boldsymbol{b} - \mathsf{K}\boldsymbol{c}$ so that $\boldsymbol{b}^T\mathsf{P}^2\boldsymbol{b} = \|\boldsymbol{b} - \mathsf{K}\boldsymbol{c}\|_2^2$. The generalized cross validation criterion is defined using this as (see [6, 15, 33])

$$\mathrm{C}_{\mathrm{GCV}} = \boldsymbol{b}^T\mathsf{P}^2\boldsymbol{b}\frac{M}{(\mathrm{trace}\,\mathsf{P})^2}. \tag{29}$$

Again, for the purposes of choosing the parameter η, we reject any η values for which K does not have full column rank.
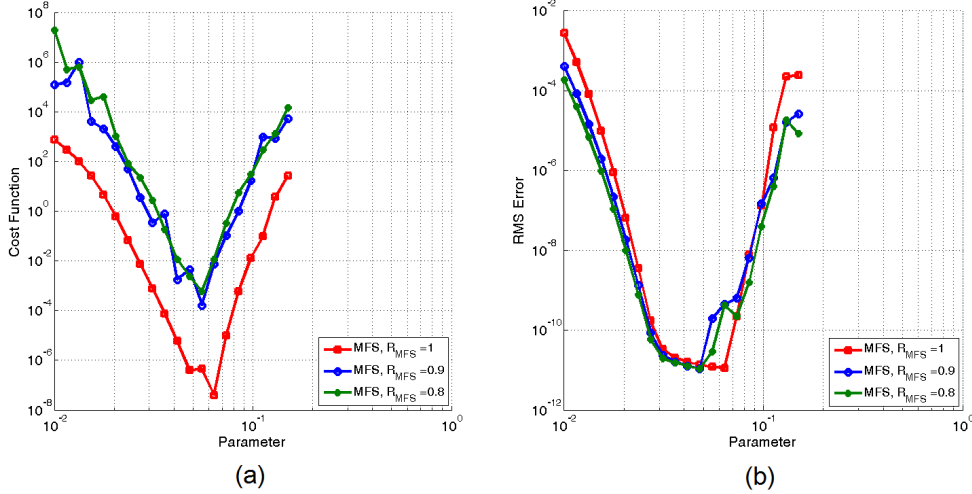
Figure 3. Spherical domain - (a) cost function and (b) error on the electric scalar potential, both as a function of the η parameter, for different values of R_{MFS}.

5. Numerical results

We approach the M/EEG forward problem by considering both a spherical domain and a realistic (one compartment) head model. FieldTrip [32] default anatomy is used in the realistic simulation and interfaces are extracted from T1-weighted MRI images by segmentation and then smoothed. The numerical computations were carried out on a workstation equipped with a six core Intel Xeon E5-2630@2.3 GHz and 24 GB of RAM. For the spherical model, the reference is the analytical solution and the domain has a radius of 0.1 m. The benchmark for the realistic geometry is a symmetric Galerkin BEM [26].

The number of unknowns both for MFS and BEM systems is N. The centers are located by a procedure of inflation of the physical inner skull surface, starting from the collocation points, randomly chosen on the inner skull surface. We take the distance η of the centers from the inner skull surface as a free parameter: the LOOCV-like procedure provides a criterion (20) which we minimize, using the MATLAB function fminbnd, to empirically choose η in an optimal way. Bounds for the parameter η are 1 (lower), 5 (upper).

We evaluate the electric scalar potential on the inner skull surface for both the spherical and the realistic homogeneous compartment model of the head ($\sigma_{brain} = 0.2$ S/m), due to a unitary current dipole that is placed at a realistic depth (≈ 1 cm from the inner skull surface). By defining the ratio between the unknowns and the collocation points, R_{MFS}, in Figure 3 we report the error on the electric scalar potential as a function of the η parameter, for different values of R_{MFS} and $N = 5000$. In the same figure, we show also the behavior of the cost function for varying η parameter. In Figure 3, it appears that the LOOCV-like cost functions predicts the *optimal η* value quite accurately. The location of the minimum of the LOOCV-like error and RMS error are quite similar. The results improve when $M \cong N$, i.e. the MFS matrix is not too *tall* and *skinny*.

In the realistic setting, a BEM reference solution is considered by referring to a fine mesh such that N is equal to 4500. In Table 1 a performance comparison among MFS, MFS with the LOOCV-like strategy and BEM for the potential problem is provided. In this case, for both

Table 1. Performance comparison among MFS, MFS with LOOCV-like and BEM for the scalar potential problem, in the realistic setting. A BEM reference solution is considered with $N = 4500$.

N	MFS		MFS LOOCV-like		BEM	
	Rel. diff.	CPU time [s]	Rel. diff.	CPU time [s]	Rel. diff.	CPU time [s]
600	2.6282e–01	3.9616e–01	1.8091e–01	2.2773e+00	3.0873e–01	1.0135e+01
993	1.5016e–01	5.9742e–01	1.2030e–01	7.5209e+00	1.6552e–01	1.6627e+01
1643	6.2979e–02	2.1083e+00	5.4633e–02	1.8293e+01	9.0817e–02	4.0212e+01
2719	6.7595e–02	9.1017e+00	4.8583e–02	3.6801e+01	6.4571e–02	1.0366e+02
4500	6.6277e–02	3.7390e+01	4.4742e–02	2.4016e+02	N/A	2.8483e+02
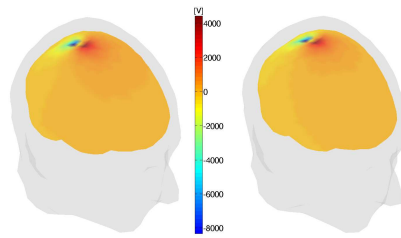
Figure 4. Electric scalar potential map: BEM (left-side), MFS with LOOCV procedure (rigth-side).

MFS approaches, we considered $R_{MFS} = 0.8$. Relative differences in 2-norm with respect to the BEM reference solution and CPU times are reported for varying N. It can be observed that the LOOCV-like procedure allows for an improvement in terms of accuracy. In fact, solutions obtained by means of the proposed strategy are slightly more accurate than the ones obtained with the standard approach; the CPU times are higher but the centers are automatically and reliably selected by means of the LOOCV-like procedure. Nevertheless, the proposed approach is competitive with the BEM approach, not just from the accuracy standpoint but also when CPU times are concerned.

In Figure 4, the electric scalar potential distributions obtained with BEM and MFS with LOOCV-like procedure, are also reported for the previously described realistic head example at the finest discretization.

6. Conclusion

The MFS is an attractive method for solving the M/EEG forward problem. It avoids complex and time consuming meshing algorithms as well as troublesome and costly numerical integration routines, without sacrificing accuracy. Results for the electric potential problem (EEG) in a realistic geometry confirmed a very good agreement with BEM reference solutions and a competitive numerical performance. As a challenging new task, we have presented a first application of an LOOCV-like strategy, for automatically determining the center locations and have obtained promising results in doing so. Future work could involve efficiently optimizing the LOOCV criteria as suggested in [29], which would be especially useful during the inverse problem solve when different inflation/deflation parameters could provide better accuracy during each forward solve. It may also be beneficial to experiment with choosing the number of source terms as part of the LOOCV process.

Acknowledgement

References

[1] G. Adde, M. Clerc, O. Faugeras, R. Keriven, J. Kybic, T. Papadopoulo, Symmetric BEM formulation for the M/EEG forward problem, in: C. Taylor, J. Noble (eds.), Information Processing in Medical Imaging, vol. 2732 of Lecture Notes in Computer Science, Springer Berlin Heidelberg, 2003, pp. 524–535.

[2] G. Ala, G. Di Blasi, E. Francomano, A numerical meshless particle method in solving the magnetoencephalography forward problem, International Journal of Numerical Modelling: Electronic Networks, Devices and Fields 25 (5-6) (2012) 428–440.

[3] G. Ala, G. Fasshauer, E. Francomano, S. Ganci, M. McCourt, A meshfree solver for the MEG forward problem, IEEE Transactions on Magnetics 51 (3) (2015) 5000304.

[4] G. Ala, G. Fasshauer, E. Francomano, S. Ganci, M. J. McCourt, The method of fundamental solutions in solving coupled boundary value problems for M/EEG, SIAM Journal on Scientific Computing 37 (4) (2015) B570–B590.

[5] G. Ala, E. Francomano, A multi-sphere particle numerical model for non-invasive investigations of neuronal human brain activity, Progress in Electromagnetics Research Letters 36 (2013) 143–153.

[6] S. Arlot, A. Celisse, A survey of cross-validation procedures for model selection, Statistics Surveys (4) (2010) 40–79.

[7] J. Belliveau, D. J. Kennedy, R. McKinstry, B. Buchbinder, R. Weisskoff, M. Cohen, Functional mapping of the human visual cortex by magnetic resonance imaging, Science 254 (1991) 716–719.

[8] S. Broeh, H. Zhou, M. Peters, Computation of neuromagnetic fields using finite-element method and Biot-Savart law, Medical and Biological Engineering and Computing 34 (1) (1996) 21–26.

[9] R. W. Brown, Y. C. Cheng, E. M. Haacke, M. R. Thompson, R. Venkatesan, Magnetic Resonance Imaging: Physical Properties and Sequence Design, Wiley Blackwell, 2014.

[10] C. Chen, A. Karageorghis, Y. Li, On choosing the location of the sources in the MFS, Numerical Algorithms (2015) 1–24.

[11] W. Chen, Z. Fu, C. Chen, Recent advances in radial basis function collocation methods, Springer, 2014.

[12] P. Craven, G. Wahba, Smoothing noisy data with spline functions, Numer. Math. 31 (4) (1979) 377–403.

[13] G. Fairweather, A. Karageorghis, The method of fundamental solutions for elliptic boundary value problems, Advances in Computational Mathematics 9 (1) (1998) 69–95.

[14] G. Fasshauer, Meshfree Approximation Methods with MATLAB, World Scientific Publishing Co., Inc., River Edge, NJ, USA, 2007.

[15] G. Fasshauer, M. McCourt, Kernel-based Approximation Methods using MATLAB, World Scientific Publishing Co., Inc., 2015.

[16] G. Fasshauer, J. Zhang, On choosing "optimal˝ shape parameters for RBF approximation, Numerical Algorithms 45 (2007) 345–368.

[17] G. H. Golub, M. Heath, W. G., Generalized cross-validation as a method for choosing a good ridge parameter, Technometrics 21 (2) (1979) 215–223.

[18] G. H. Golub, C. F. Van Loan, Matrix computations, vol. 3, JHU Press, 2012.

[19] H. Hallez, B. Vanrumste, R. Grech, J. Muscat, W. De Clercq, A. Vergult, Y. D'Asseler, K. P. Camilleri, S. G. Fabri, S. Van Huffel, I. Lemahieu, Review on solving the forward problem in EEG source analysis, Journal of NeuroEngineering and Rehabilitation 4 (46) (2007) 1–29.

[20] M. Hämäläinen, R. Hari, R. Ilmoniemi, J. Knuutila, O. Lounasmaa, Magneto-encephalography—theory, instrumentation, and applications to noninvasive studies of the working human brain, Reviews of Modern Physics 65 (2) (1993) 413–497.

[21] M. Hämäläinen, J. Sarvas, Realistic conductivity geometry model of the human head for interpretation of neuromagnetic data, IEEE Transactions on Biomedical Engineering 36 (2) (1989) 165–171.

[22] B. He, T. Musha, Y. Okamoto, S. Homma, Y. Nakajima, T. Sato, Electric dipole tracing in the brain by means of the boundary element method and its accuracy, IEEE Transactions on Biomedical Engineering 34 (6) (1987) 406–414.

[23] R. Johnston, G. Fairweather, The method of fundamental solutions for problems in potential flow, Applied Mathematical Modelling 8 (4) (1984) 265–270.

[24] W. A. Kalender, Computed Tomography: Fundamentals, System Technology, Image Quality, Applications, Wiley Online Library, 2011.

[25] G. Knoll, Single-photon emission computed tomography, Proceedings of the IEEE 71 (3) (1983) 320–329.

[26] J. Kybic, M. Clerc, T. Abboud, O. Faugeras, R. Keriven, T. Papadopoulo, A common formalism for the integral formulations of the forward EEG problem, IEEE Transactions on Medical Imaging 24 (1) (2005) 12–28.

[27] M. Li, C. Chen, A. Karageorghis, The MFS for the solution of harmonic boundary value problems with non-harmonic boundary conditions, Comput. Math. Appl. 66 (2013) 2400–2424.

[28] R. Mathon, R. Johnston, The approximate solution of elliptic boundary value problems by fundamental solutions, SIAM Journal on Numerical Analysis 14 (4) (1977) 638–650.

[29] M. McCourt, I. Dewancker, S. Ganci, Preemptive termination of suggestions during sequential kriging optimization of a brain activity reconstruction simulation, in: NIPS BayesOpt Workshop, 2016, https://bayesopt.github.io/papers/2016/Mccourt.pdf.

[30] J. Nocedal, S. Wright, Numerical optimization, Springer Science & Business Media, 2006.

[31] J. Ollinger, J. Fessler, Positron-emission tomography, IEEE Signal Processing Magazine 14 (1) (1997) 43–55.

[32] R. Oostenveld, P. Fries, E. Maris, J. Schoffelen, FieldTrip: open source software for advanced analysis of MEG, EEG, and invasive electrophysiological data, Computational intelligence and neuroscience 2011 (2011) 1–9.

[33] M. Orr, Introduction to radial basis function networks, Technical Report - University of Edinburgh - Centre for Cognitive Sciences (1996) 1–67.

[34] C. Piret, The orthogonal gradients method: A radial basis functions method for solving partial differential equations on arbitrary surfaces, Journal of Computational Physics 231 (14) (2012) 4662–4675.

[35] S. Rippa, An algorithm for selecting a good value for the parameter c in radial basis function interpolation, Advances in Computational Mathematics 11 (23) (1999) 193–201.

[36] J. Sarvas, Basic mathematical and electromagnetic concepts of the biomagnetic inverse problem, Physics in Medicine and Biology 32 (1) (1987) 11.

[37] R. Schaback, All well-posed problems have uniformly stable and convergent discretizations, Numerische Mathematik 132 (3) (2016) 597–630.

[38] M. Stenroos, A. Hunold, J. Haueisen, Comparison of three-shell and simplified volume conductor models in magnetoencephalography, NeuroImage 94 (2014) 337–348.

[39] F. Tadel, S. Baillet, J. Mosher, D. Pantazis, R. Leahy, Brainstorm: a user-friendly application for MEG/EEG analysis, Computational intelligence and neuroscience 2011 (2011) 8.

[40] O. Tanzer, S. Jarvenpaa, J. Nenonen, E. Somersalo, Representation of bioelectric current sources using whitney elements in the finite element method, Physics in Medicine and Biology 50 (13) (2005) 3023–3039.

[41] N. von Ellenrieder, C. Muravchik, A. Nehorai, A meshless method for solving the EEG forward problem, IEEE Transactions on Biomedical Engineering 52 (2) (2005) 249–257.

[42] C. Wolters, H. Köstler, C. Möller, J. Härdtlein, L. Grasedyck, W. Hackbusch, Numerical mathematics of the subtraction method for the modeling of a current dipole in EEG source reconstruction using finite element head models, SIAM Journal on Scientific Computing 30 (1) (2008) 24–45.

[43] C. Wolters, M. Kuhn, A. Anwander, S. Reitzinger, A parallel algebraic multigrid solver for finite element method based source localization in the human brain, Computing and Visualization in Science 5 (3) (2002) 165–177.

[44] Y. Yan, P. Nunez, R. Hart, Finite-element model of the human head: scalp potentials due to dipole sources, Medical and Biological Engineering and Computing 29 (5) (1991) 475–481.

[45] A. Zeynep, G. Gençer, An advanced boundary element method (BEM) implementation for the forward problem of electromagnetic source imaging, Physics in Medicine and Biology 49 (21) (2004) 5011–5028.